# The Effect of Isolator Mobility in Base Isolation Systems Optimized by Accounting for Soil-Structure Interaction

Ayla Ocak[1][0000-0003-2236-7834], Sinan Melih Nigdeli[2][0000-0002-9517-7313] and Gebrail Bekdaş[2][0000-0002-7327-9810]

[1] Istanbul Gelisim University, 34310 Istanbul, Turkey
ayocak@gelisim.edu.tr
[2] Istanbul University - Cerrahpaşa, 34320 Istanbul, Turkey
melihnig@iuc.edu.tr, bekdas@iuc.edu.tr

**Abstract.** Seismic base isolators are highly effective control systems that rapidly reduce the acceleration of seismic vibrations transmitted to a structure. Key factors to consider in the seismic isolation of a structure include the region's soil conditions and seismicity. This study focuses on investigating changes in a structure's dynamic response based on different isolator mobility levels for two soil conditions, soft and dense, in the seismic isolation of a structure located in a region exposed to distant fault earthquakes. To conclude, the Jaya algorithm, a metaheuristic algorithm, was used to optimize the system period and damping ratio characteristics of an isolator-equipped structure subjected to a FEMA far-fault earthquake for both soft and dense soil conditions, considering different isolator mobility levels. In the optimization, FEMA earthquake records known to be critical for both soft and dense soil conditions were considered for the given structural characteristics. Critical earthquake analyses were performed using the obtained optimal isolator system parameters, and the effect of isolator mobility on the damping of earthquake vibrations was investigated for both soft and dense soil types. Earthquake analyses have shown that taking the SSI effect into account in an isolator-based system can increase the system's required isolator mobility for a given damping ratio and that, when isolator mobility is increased relatively, the system's required period can be reduced.

**Keywords:** Seismic Base Isolation, Structural Control, Soil-Structure Interaction, Optimization.

## 1 Introduction

Base isolators are effective control devices that reduce a structure's dynamic responses by damping strong vibrations, such as those caused by earthquakes. They play an active role, particularly in minimizing the transmission of vibrations such as seismic vibrations, which threaten structural safety and negatively impact human life. It is well established that the fundamental operating principle of seismic isolators is to interrupt and reduce the transmission of vibrations that could be transmitted from the ground to the structure through oscillations generated at the isolator level. Their high performance

in reducing acceleration sets seismic isolators apart from similar control devices. Isolators typically achieve this effect by extending the structure's natural period. There are two key parameters for an isolator to be added to a structure. These are the control system period, which allows the structure to oscillate in order to prevent damage caused by vibrations to the superstructure, and the system damping ratio, which affects the isolator's ductility when seismic energy is transmitted. The optimal tuning of these parameters is crucial for reducing the structure's dynamic responses, such as maximum displacement and total acceleration. In the optimization of base isolators, the rubber type, elastomer layer dimensions, allowable isolator displacement, period, damping ratio, isolator stiffness, the normalized yield strength of the lead core, the yield deformation of the lead-rubber bed, the yield base shear ratio, the coefficient of friction, the radius of curvature, the number of isolators, and their arrangement have been optimized in various studies [1–7]. The type of isolator selected and its characteristic damping properties play a significant role in determining which parameters to optimize. The vast majority of studies on control devices represent research that does not account for structure-soil interaction. However, it has been observed that soil typology affects the isolator's design parameters, shear displacement, and the acceleration accumulated in the structure [8]. Furthermore, a structure on soft ground is affected by structural motion and soil stiffness during an earthquake and must accommodate significant displacement demands [8–10]. The influence of the soil on a control system to be installed in the structure has been supported by various studies [11–15]. All of the findings obtained highlight the need to incorporate the structure-soil interaction into control system designs and to integrate control systems into the structure, taking into account not only the region's seismicity but also the soil conditions.

The seismic base isolator evaluated in this study is linearized, and its two fundamental parameters, period and damping ratio, have been optimized. Meta-heuristic algorithms have gained prominence in the literature as a method frequently preferred in recent years for the optimization process. Meta-heuristic algorithms are known to be mathematical models with an infrastructure that mimics natural phenomena and instinctive animal behavior, inspired by nature. In studies on the design of optimal control systems for base isolators, meta-heuristic algorithms such as the harmony search algorithm, a derivative aimed at finding the best harmony [2, 16] the genetic algorithm inspired by natural selection and evolutionary processes [3, 7, 17], particle swarm optimization inspired by the swarm behavior of birds, fish, and similar organisms [4, 18], and the grasshopper optimization algorithm [5, 19], inspired by the swarm interactions and movements of grasshoppers, have been preferred. Within the scope of this study, the Jaya algorithm [20], a good optimization tool due to its speed in reaching the optimal solution and its simple structure, was used. Jaya is an algorithm that aims to find the best solutions by moving away from poor solutions; it features a simple and easy-to-understand structure, contains a single solution-generation equation, and does not involve any algorithmic steps.

Within the scope of this study, a 50% damped seismic isolator was placed on the base of a structure for two types of soil (soft and dense) and optimized using the Jaya algorithm for isolator displacement limits of 30 and 40 cm. The structural model used by Ocak et al. [12] was adopted for the optimization. In a study by Ocak et al. [21],

which optimized a structural model without accounting for soil-structure interaction (SSI), it was found that for a system equipped with isolators having 50% damping, the best control performance was achieved with an isolator displacement limit of 30 cm, followed by the system with a 40 cm limit. Consequently, the present study aims to investigate whether the inclusion of SSI effects makes a significant difference when the isolator displacement capacity is set to 30 cm or 40 cm. The NORTHR/MUL279 and DUZCE/BOL090 earthquakes identified by Ocak et al. [12] as critical for soft and dense soils, respectively, in a 50% damped system were applied to the structure using FEMA P-695 [22] earthquake records. The structural properties were defined in the Matlab [23] program, and the selected critical earthquakes were applied to the structure via Matlab Simulink. The damping ratio and period of the isolated system were optimized to minimize the structure's total acceleration. In the critical earthquake analyses performed using the obtained optimal parameters, the effect of isolator mobility on control performance was evaluated for a 50% damped system on soft and dense soils.

# 2 Methodology

## 2.1 Design of a Structure with Soil-Structure Interaction and Seismic Base Isolator

Seismic isolators are vibration-damping systems designed to reduce structural acceleration and displacement. In the design of a seismically isolated structure that accounts for structure-soil interaction (SSI), various parameters representing the soil's influence are included. Figure 1 shows the mathematical model of a multi-story structure that accounts for structure-soil interaction.

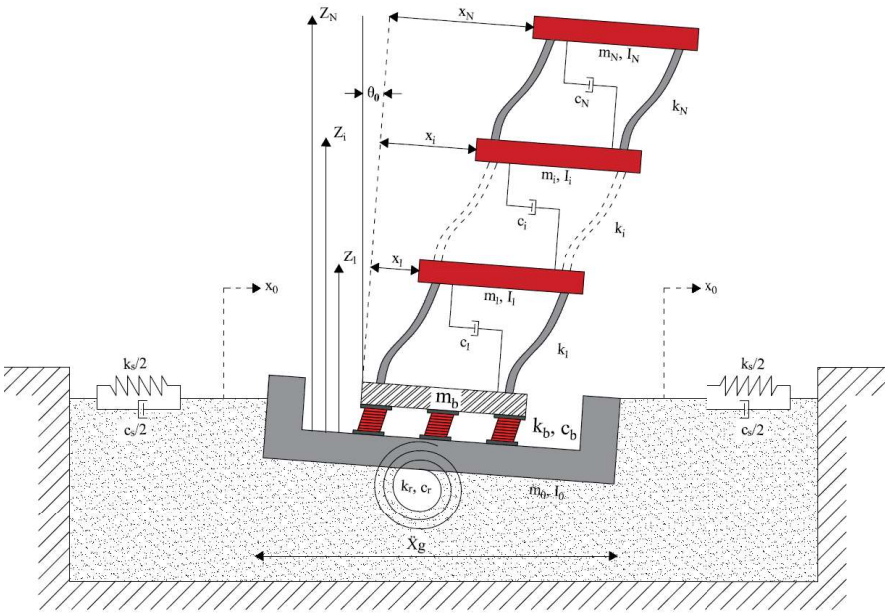



**Fig. 1.** A structural model of a base-isolated multi-story building that accounts for SSI effects.

In Figure 1, the index "*b*" represents the properties of the isolator, "*i*" represents the floor number, "*z*" represents the floor heights, and "*N*" represents the number of the topmost floor of the structure; the structure has floors ranging from $i = 1$ to $N$. "I" represents the floor inertia, "*m*" represents the mass, "*k*" represents the stiffness, and "*c*" represents the damping coefficient. The mass and stiffness of the foundation are denoted by "$m_0$" and "$I_0$," respectively. The floor's swaying is denoted by the index "s," and its rocking by the index "r." The floor's swaying stiffness and damping coefficient are denoted by $k_s$ and $c_s$, respectively, while the floor's rocking stiffness and damping coefficient are denoted by $k_r$ and $c_r$. The total mass of the structure ($m_{total}$) is calculated by summing the mass of the isolator ($m_b$) and the total mass of the structure ($m_{structure}$), as shown in Equation 1. The mass of the isolator story is assumed to be equal to the mass of one story of the structure.

$$m_{total} = m_b + m_{structure} \tag{1}$$

It alters the system's degrees of freedom, natural period, stiffness, and damping calculations. In a single-degree-of-freedom (SDOF) system, the isolator and structure move together, exhibiting common stiffness, natural period, and damping. For a single-degree-of-freedom (SDOF) structure with an isolator, the system's period ($T_b$) is given in Equation 2, its stiffness ($k_b$) in Equation 3, and its damping coefficient $c_b$) in Equation 4. In these equations, the system's damping ratio is denoted by $\zeta_b$ and its natural angular frequency by $w_b$.

$$T_b = \frac{2\pi}{w_b} \tag{2}$$

$$k_b = m_{total} \times w_b^2 \tag{3}$$

$$c_b = 2 \times \zeta_b \times m_{total} \times w_b \tag{4}$$

The elements representing the system's behavior under structure-soil interaction are presented in a matrix in Equation 5. $X(t)$ denotes the system's displacement, and $N$ denotes the floor number.

$$X(t) = \begin{bmatrix} X_b \\ X_1 \\ X_2 \\ \vdots \\ X_{N-1} \\ X_N \\ X_0 \\ \theta_0 \end{bmatrix} \tag{5}$$

The matrix containing the layer masses ($M_v$) is shown in Equation 6, the matrix obtained by multiplying these by the layer heights ($MZ$) is shown in Equation 7, and the mass matrix ($m^*$) multiplied by the ground acceleration in the fundamental equation of motion is shown in Equation 8.

$$[M_v] = \begin{bmatrix} m_b \\ m_1 \\ m_2 \\ \vdots \\ m_{N-1} \\ m_N \end{bmatrix} \tag{6}$$

$$[MZ] = \begin{bmatrix} m_b z_1 \\ m_1 z_1 \\ m_2 z_2 \\ \vdots \\ m_{N-1} z_{N-1} \\ m_N z_N \end{bmatrix} \tag{7}$$

$$m^* = \begin{bmatrix} m_b \\ m_1 \\ m_2 \\ \vdots \\ m_{N-1} \\ m_N \\ m_0 + m_b + \left(\sum_{i=1}^{N} m_i\right) \\ \left(\sum_{i=1}^{N} m_i z_i\right) + m_b z_1 \end{bmatrix} \tag{8}$$

The mass, stiffness, and damping matrices $M$, $K$, and $C$ of the isolated system are given in Equation 9, Equation 10, and Equation 11, respectively. In its simplest form, the motion is formulated in Equation 12.

$$[M]=\begin{bmatrix}[M_f] & [M_v] & [MZ]\\ [M_v]^T & m_0+m_b+\left(\sum_{i=1}^{N} m_i\right) & \left(\sum_{i=1}^{N} m_i z_i\right)+m_b z_1\\ [MZ]^T & \left(\sum_{i=1}^{N} m_i z_i\right)+m_b z_1 & \left(\sum_{i=1}^{N} m_i {z_i}^2\right)+m_b {z_1}^2 I_0+I_b+\sum_{i=1}^{N} I_i\end{bmatrix} \quad (9)$$

$$[K]=\begin{bmatrix}[K_f] & 0 & 0\\ 0\ldots 0 & k_s & 0\\ 0\ldots 0 & 0 & k_r\end{bmatrix} \quad (10)$$

$$[C]=\begin{bmatrix}[C_f] & 0 & 0\\ 0\ldots 0 & c_s & 0\\ 0\ldots 0 & 0 & c_r\end{bmatrix} \quad (11)$$

$$[M]\ddot{X}(t)+[C]\dot{X(t)}+[K]X(t)=-[m^*]\ddot{X}_g \quad (12)$$

In the equations, the gravitational acceleration is denoted by $\ddot{X}_g$, the displacement of the system by $X(t)$, the velocity by $\dot{X(t)}$, and the acceleration by $\ddot{X}(t)$. The values $M_f$, $K_f$, and $C_f$ represent the mass, stiffness, and damping coefficient matrices that result when an isolator system is added to a fixed-base structure.

## 2.2 Optimization with Jaya Algorithm

The Jaya algorithm [20], developed by Rao, is a meta-heuristic algorithm that generates new solutions based on the best and worst results relative to the objective function during the solution search process. Since it does not involve any algorithmic factors, it quickly reaches the optimal solution. It generates solution vectors using a single solution-generation equation. Equation 13 presents the solution-generation equation for the Jaya algorithm.

$$X_{i,new} = X_{i,j} + rand(X_{i,best} - |X_{i,j}|) - rand(X_{i,worst} - |X_{i,j}|) \quad (13)$$

In the equation, each new candidate solution is denoted by $X_{i,new}$. After the initial solution matrix is constructed, the best and worst solutions in the solution matrix, based on the objective function, are denoted by $X_{i,best}$ and $X_{i,worst}$, respectively. The jth candidate solution for the ith variable is denoted by $X_{i,j}$.

The objective of the optimal design of an isolator-based system subjected to SSI is to minimize the maximum total acceleration transmitted to the superstructure. The system's displacement is constrained as shown in Equation 14 to protect the isolator from deformation caused by large displacements. The objective function of the problem is shown in Equation 15.

$$g(x) = \max(|X|) \quad (14)$$

$$f(x) = Minimize\left(\max\left(\left|\ddot{X}\right|\right)\right) \quad (15)$$

## 3 Numerical Example

In this study, based on the example structural model shown in Figure 1, a single-degree-of-freedom structural model was used in which the superstructure was assumed to be rigid and to move in unison with the isolator. Two cases were investigated in which the structure was located on soft and dense soil types with two degrees of freedom. Optimal design parameters were obtained for the structure with a damper limit of 50% and displacement limits of 30 and 40 cm under the critical displacement record. The critical earthquake records were selected from the FEMA earthquake records identified as critical for soft and dense soil types in the studies by Ocak et al. [12], which used the same 10-story structural model for a system with 50% damping. For soft soil, this is the NORTHR/MUL279 earthquake that occurred in 1994, and for dense soil, it is the DUZCE/BOL090 earthquake record that occurred in 1999. The structural model properties were taken from the study by Liu et al. [24]. The floor-to-floor height of the structure was set at 4 m, the floor mass at 980 metric tons, and the foundation mass at 1,960 metric tons. The isolator and floor inertia moments were set at $1.31 \times 10^8$ kg·m², and the foundation inertia moment at $1.96 \times 10^8$ kg·m². The stiffness between the first and tenth floors of the structure ranges from 2,130 to 1,870 MN/m, while the damping coefficient ranges from 42.6 to 34.7 MNs/m. The soil properties used in the study are presented in Table 1.

**Table 1.** Soil and foundation characteristics [24].

| Soil Type | $c_s$ (Ns/m) | $k_s$ (N/m) | $k_r$ (N/m) | $c_r$ (Ns/m) |
|---|---|---|---|---|
| Soft Soil | $2.19x10^8$ | $1.91x10^9$ | $7.53x10^{11}$ | $2.26x10^{10}$ |
| Dense Soil | $1.32x10^9$ | $5.75x10^{10}$ | $1.91x10^{13}$ | $1.15x10^{11}$ |

The Jaya algorithm was used to optimize the structure. During optimization, the system period with isolators was optimized within the range of 1–5 s, and the damping ratio was optimized within the range of 1–50%. The population size was set to 10, the number of iterations to 1,000, and the isolator displacement limits to 30 and 40 cm. The optimum parameters obtained from optimization are presented in Table 2. The displacement and total acceleration values of the structure, derived from the critical seismic analysis performed for soft and dense soil conditions using these optimum parameters, are shown in Table 3.

The displacement and total acceleration plots for the isolated system corresponding to a 40 cm displacement limit, which yielded the best results for both soft and dense soil, are presented in Figure 2 and Figure 3, respectively.

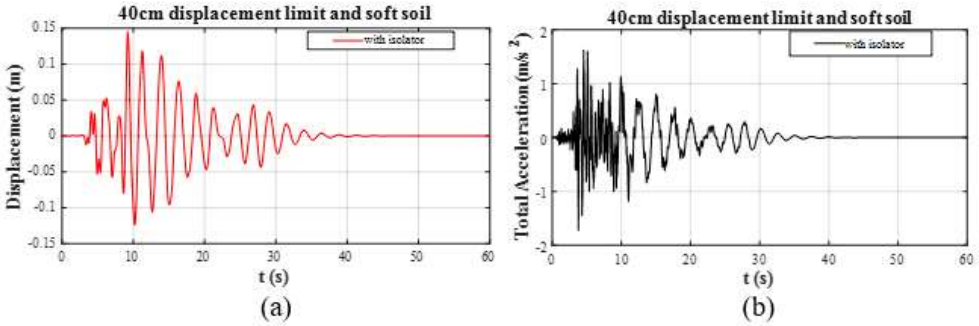



**Fig. 2.** Analysis plots for soft soil for a system with a 40 cm displacement limit, subjected to the NORTHR/MUL279 earthquake record: (a) Structural displacement, (b) Total structural acceleration.

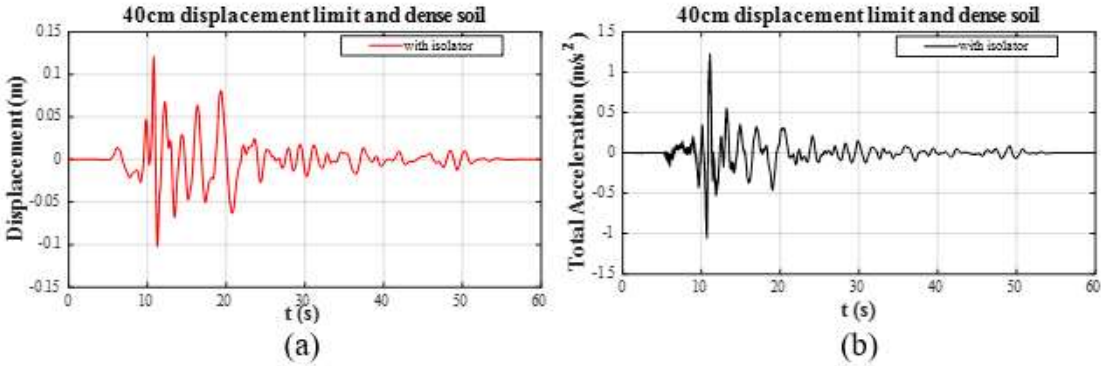



**Fig. 3.** Analysis plots for dense soil a system with a 40 cm displacement limit, subjected to the DUZCE/BOL090 earthquake record: (a) Structural displacement, (b) Total structural acceleration.

**Table 2.** Optimum parameters.

| Soil Type | | Isolator movement limit | |
|---|---|---|---|
| | | 30cm | 40cm |
| Soft Soil | $\zeta_b$ | 0.0604 | 0.1533 |
| | $T_b$ (s) | 2.8927 | 2.1512 |
| Dense Soil | $\zeta_b$ | 0.1313 | 0.5000 |
| | $T_b$ (s) | 5 | 3.6485 |

**Table 3.** Optimum responses.

| Soil Type | Limit | Displacement (m) | | Total Acceleration ($m/s^2$) | |
|---|---|---|---|---|---|
| | | Without isolator | With isolator | Without isolator | With isolator |
| Soft Soil | 30cm | 0.2112 | 0.1724 | 6.5254 | 1.0799 |
| | 40cm | | 0.1454 | | 1.7259 |
| Dense Soil | 30cm | 0.3264 | 0.2020 | 16.7801 | 0.4863 |
| | 40cm | | 0.1211 | | 1.2278 |

## 4 Discussion and Conclusions

In this study, an investigation was conducted into the effect of isolator mobility on control performance when the structure-soil interaction (SSI) effect is taken into account, using a single-degree-of-freedom (SDOF) structure model in which the superstructure is assumed to be rigid. In a previously tested structural model [21], for a system with 50% damping, when the SSI effect was not considered, a 30 cm isolator displacement was sufficient for the different displacement capacities of 30, 40, and 50 cm isolators; in this study, however, the contribution of the SSI effect to control performance was investigated for isolator movement limits of 30 cm and 40 cm, which had yielded the best results without the SSI effect. In this study, an investigation was conducted into the effect of isolator mobility on control performance when the structure-soil interaction (SSI) effect is taken into account, using a single-degree-of-freedom (SDOF) structure model in which the superstructure is assumed to be rigid. In

a previously tested structural model, for a system with 50% damping, when the SSI effect was not considered, a 30 cm isolator displacement was sufficient for the different displacement capacities of 30, 40, and 50 cm isolators; in this study, however, the contribution of the SSI effect to control performance was investigated for isolator movement limits of 30 cm and 40 cm, which had yielded the best results without the SSI effect. For an isolator displacement capacity of 40 cm, the total acceleration of the structure decreased by 73% for soft soil and by 92% for dense soil. At a displacement limit of 30 cm, the total acceleration of the isolated system decreased by 83% for soft soil and by 97% for dense soil. A 40 cm displacement capacity proved more effective in reducing acceleration, while a 30 cm displacement limit was more effective in reducing displacement. The findings indicate that accounting for the SSI effect in an isolator-based system can increase the system's required isolator displacement for a given damping ratio compared to a scenario where the SSI effect is not considered; conversely, the SSI effect can reduce the required period in a system with relatively greater isolator displacement limit. In the optimization performed for the isolator-based system, the required system period was longer for both soil types in the 30 cm limited system, which has relatively lower mobility. As the isolator's mobility limit increased, the required period decreased, but the demand for damping ratio increased. The findings indicate that accounting for the SSI effect in an isolator-based system can increase the system's required isolator displacement for a given damping ratio compared to a scenario where the SSI effect is not considered; conversely, the SSI effect can reduce the required period in a system with relatively greater isolator displacement.

## References


1. Léger, N., Rizzian, L., & Marchi, M. (2017). Reliability-based design optimization of reinforced concrete structures with elastomeric isolators. *Procedia engineering*, *199*, 1193-1198.
2. Ocak, A., Bekdaş, G., & Nigdeli, S. M. (2024). Optimum design of hybrid base isolation and tuned liquid damper systems for structures under near-fault ground motions. *ASCE-ASME Journal of Risk and Uncertainty in Engineering Systems, Part A: Civil Engineering*, *10*(4), 04024061.
3. Charmpis, D. C., Komodromos, P., & Phocas, M. C. (2012). Optimized earthquake response of multi-storey buildings with seismic isolation at various elevations. *Earthquake Engineering & Structural Dynamics*, *41*(15), 2289-2310.
4. Ghosh, S. K., Kashyap, I., & Das, D. (2026). Machine learning-enhanced metaheuristic optimization of lead rubber bearings for inter-story isolated buildings under seismic load. *ENGINEERING Structure and Civil Engineering*, *20*(1), 36-79.
5. Mehri, F., Mollaei, S., Farsangi, E. N., Babaei, M., & Ghahramani, F. (2023). Application of a novel optimization algorithm in design of lead rubber bearing isolation systems for seismic rehabilitation of building structures. *International Journal of Engineering, Transactions C: Aspects*, *36*(3), 594-603.
6. Tsipianitis, A., Spachis, A., & Tsompanakis, Y. (2022). Combined optimization of friction-based isolators in liquid storage tanks. *Applied Sciences*, *12*(19), 9879.
7. El Ouardani, A., & Tbatou, T. (2024). Seismic isolators layout optimization using genetic algorithm within the pymoo framework. *Civil Engineering Journal*, *10*(8), 2517-2535.

8. Radkia, S., Rahnavard, R., Tuwair, H., Gandomkar, F. A., & Napolitano, R. (2020, October). Investigating the effects of seismic isolators on steel asymmetric structures considering soil-structure interaction. In *Structures* (Vol. 27, pp. 1029-1040). Elsevier.
9. Spyrakos, C. C., Maniatakis, C. A., & Koutromanos, I. A. (2009). Soil–structure interaction effects on base-isolated buildings founded on soil stratum. *Engineering Structures*, *31*(3), 729-737.
10. Kelly, J. M. (1991). *Shake table tests of long period isolation system for nuclear facilities at soft-soil sites*. Argonne National Laboratory.
11. Fosoul, S. A., & Tait, M. J. (2021). Soil-pile-structure interaction effects on seismic demands and fragility estimates of a typical Ontario highway bridge retrofitted with fiber reinforced elastomeric isolator. *Soil Dynamics and Earthquake Engineering*, *151*, 106967.
12. Ocak, A., Nigdeli, S. M., & Bekdaş, G. (2023, October). Optimization of the base isolator systems by considering the soil-structure interaction via metaheuristic algorithms. In *Structures* (Vol. 56, p. 104886). Elsevier.
13. Jasim, F. A., Jasim, N. A., & Al-Hussein, A. A. (2024). Assessment of Soil-Structure Interaction Effects on Seismic Behavior of Isolator and Mass Damper Equipped Buildings. *Mathematical Modelling of Engineering Problems*, *11*(2), 325.
14. Öner, E., Aydoğan, A., Yurdakul, M., Ergün, M., & Artar, M. (2026). Seismic performance of prestressed girder bridges considering soil-pile-structure interaction and isolation systems. *Structural Engineering and Mechanics*, *97*(2).
15. Mellas, N., Mellas, M., Mabrouki, A., Hebbache, K., & Alemdar, Z. F. (2026). A novel study on seismic response of base-isolated wind turbine taking the soil-structure interaction impact. *Marine Georesources & Geotechnology*, *44*(5), 1178-1195.
16. Geem, Z.W., Kim, J.H., Loganathan, G.V.: A new heuristic optimization algorithm: harmony search, Simulation, 76(2), 60-68 (2001).
17. Holland, J.H.: Adaptation in Natural and Artificial Systems, University of Michigan Press, Ann Arbor, MI (1975).
18. Kennedy, J., Eberhart, R. C.: Particle swarm optimization, Proceedings of IEEE International Conference on Neural Networks No. IV, 27 November–1 December Perth, IEEE Service Center, Piscataway, NJ, 1942–1948 (1995).
19. Saremi, S., Mirjalili, S., & Lewis, A. (2017). Grasshopper optimisation algorithm: theory and application. *Advances in engineering software*, *105*, 30-47.
20. Rao, R. V. (2016). Jaya: A simple and new optimization algorithm for solving constrained and unconstrained optimization problems. *International Journal of Industrial Engineering Computations*, *7*, 19-34.
21. Ocak, A., Nigdeli, S. M., Bekdaş, G., Kim, S., & Geem, Z. W. (2022). Optimization of seismic base isolation system using adaptive harmony search algorithm. *Sustainability*, *14*(12), 7456.
22. FEMA P-695. Quantification of Building Seismic Performance Factors. Washington.
23. MathWorks Inc., 2018, MATLAB R2018a. Natick, MA, USA.
24. Liu, M. Y., Chiang, W. L., Hwang, J. H., & Chu, C. R. (2008). Wind-induced vibration of a high-rise building with tuned mass damper including soil-structure interaction. *Journal of Wind Engineering and Industrial Aerodynamics*, *96*(6-7), 1092-1102.